PAPER

# Error Probability Analysis in Reduced State Viterbi Decoding

**Carlos VALDEZ†, *Nonmember*, Hiroyuki FUJIWARA†, Ikuo OKA†† *and* Hirosuke YAMAMOTO†††, *Members***

**SUMMARY** The performance evaluation by analysis of systems employing Reduced State Viterbi decoding is addressed. This type of decoding is characterized by an inherent error propagation effect, which yields a difficulty in the error probability analysis, and has been usually neglected in the literature. By modifying the Full State trellis diagram, we derive for Reduced State schemes, new transfer function bounds with the effects of error propagation. Both the Chernoff and the tight upper bound are applied to the transfer function in order to obtain the bit error probability upper bound. Furthermore, and in order to get a tighter bound for Reduced State decoding schemes with parallel transitions, the pairwise probability of the two sequences involved in an error event is upper bounded, and then the branch metric of a sequence taken from that bound is associated with a truncated instead of complete Gaussian noise probability density function. To support the analysis, particular assessment is done for a Trellis Coded Modulation scheme.

***key words:*** *reduced state decoding, viterbi algorithm, feedback equalization, intersymbol interference, trellis coded modulation*

## 1. Introduction

The development of Reduced State (RS) systems using Viterbi decoding, designed for operation in channels affected by linear Intersymbol Interference (ISI) and Additive White Gaussian Noise (AWGN), is a current subject of active research.[1]-[4] Even though Maximum Likelihood Sequence Estimation (MLSE) or equivalently Full State (FS) decoding, provides the optimum theoretical performance,[5]-[7] its practical realization may become highly complex. This is based on the fact that an ISI channel modeled as a finite state machine (fsm) has $N_{ch}=2^{mu}$ states, being $m$ the number of input bits to the system, and $u$ the channel's memory length. A coded scheme with $N_e=2^{\nu-1}$ states ($\nu$ is the code constraint length) increases further this number resulting $N=N_e \cdot N_{ch}$ states. $N$ is also the number of states of the so called *super-encoder*, and of the trellis diagram for FS decoding. On the other hand, RS schemes share an error propagation characteristic which arises from erroneous decision feedback.[8] Its effect is not serious however, since each path uses feedback decisions taken on its own record (an example of a single feedback decision provided for all the competing paths would be a Decision Feedback Equalization (DFE) block placed in front of the Viterbi decoder.[1]-[4] In the literature,[1]-[4] the performance of RS schemes has been judged basically by simulations and somewhat coarse theoretical approximations such as the minimum distance criterion. In a recent work, neglection of the error propagation effect has been justified to simplify union bound calculations by algorithmic means.[9]

The main purpose of this paper, is to present an analytical method to evaluate the performance of Reduced State (RS) systems, including the small but finite error propagation effect caused during Viterbi decoding. The organization of the paper is as follows. Section 2 introduces the system model used in the subsequent analysis. We are concerned in particular with Trellis Coded Modulation (TCM)[10] schemes, though the analysis is quite general. We derive error probability transfer function bounds for RS schemes incorporating the error propagation effect and give a simple example in Sect. 3. Section 4 deals with the attainment of tighter bounds for systems with parallel transitions in the decoder trellis. To support the analysis, simulation and theoretical results are shown in Sect. 5. Finally, we summarize our conclusions in Sect. 6.

## 2. System Model

The system model block diagram is shown in

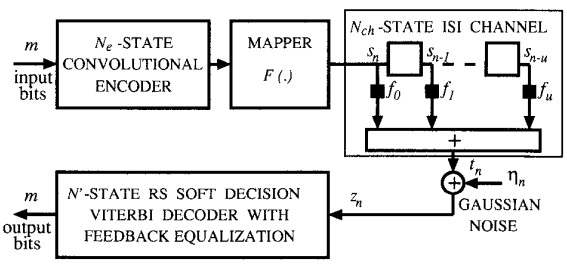


Fig. 1 System model.

Manuscript received October 30, 1992.

† The authors are with the Faculty of Electro-Communications, University of Electro-Communications, Chofu-shi, 182 Japan.

†† The author is with the Faculty of Engineering, Osaka City University, Osaka-shi, 558 Japan.

††† The author is with the Faculty of Engineering, The University of Tokyo, Tokyo, 113 Japan.

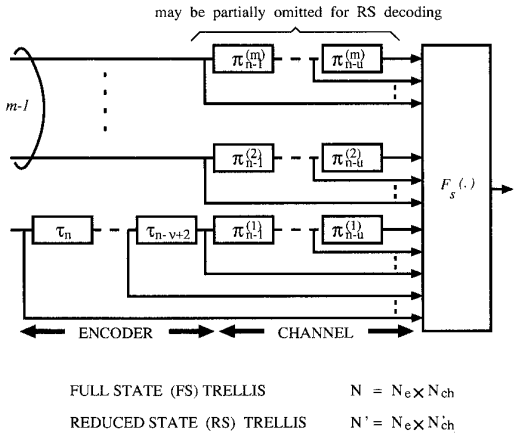


Fig. 2 General super-encoder.

Fig. 1. As seen, $m$ input bits are, upon codification, mapped by $F(\cdot)$ into a channel symbol $s_n$, which forms a received sample vector $z_n$ with $u$ preceding symbols embodied in the ISI channel output vector $t_n$, and the Gaussian noise vector $\eta_n$ (the subindex $n$ stands for time instant). The ISI weights are denoted by $f_0, f_1, \cdots, f_u$. Uncoded schemes and coded systems with mappers having non-redundant or redundant symbol alphabets (the latter case corresponds to TCM) may be viewed as particular cases. Now, for the special case of TCM, the $N_e$-state convolutional encoder with mapper $F(\cdot)$, and the $N_{ch}$-state channel of Fig. 1 are combined resulting the $N=N_e \cdot N_{ch}$-state super-encoder with modified mapper $F_s(\cdot)$ (which outputs symbol vectors $t_n$ corrupted by ISI) of Fig. 2. A FS trellis state will be given by $\alpha_n=(\sigma_n;\mu_n)$, where $\sigma_n$ and $\mu_n$ denote the encoder and the channel states, respectively. Thus,

$$\sigma_n=(\tau_n, \tau_{n-1}, \cdots, \tau_{n-\nu+2}) \tag{1}$$

$$\mu_n=(\Pi_{n-1};\Pi_{n-2};\cdots;\Pi_{n-u}) \tag{2}$$

$$\Pi_{n-k}=(\pi^{(1)}_{n-k}, \pi^{(2)}_{n-k}, \cdots, \pi^{(m)}_{n-k}) \quad k=1, 2, \cdots, u \tag{3}$$

Then, for a RS trellis state, we set a super-encoder state as $\tilde{\alpha}_n=(\sigma_n;\tilde{\mu}_n)$ such that

$$\tilde{\mu}_n=(\tilde{\Pi}_{n-1};\tilde{\Pi}_{n-2};\cdots;\tilde{\Pi}_{n-u}) \tag{4}$$

$$\tilde{\Pi}_{n-k}=(\pi^{(1)}_{n-k}, \pi^{(2)}_{n-k}, \cdots, \pi^{(m_k)}_{n-k}) \quad k=1, 2, \cdots, u \tag{5}$$

The parameter $m_k$ $(0 \leqq m_k \leqq m)$, determines the channel states reduction extent. While $m_k=0$ means complete disregard of a channel state, $m_k=m$ indicates complete knowledge of it. Partial knowledge of the same is given then by $1 \leqq m_k < m-1$. Thus, $(m_1=m_2=\cdots=m_u=m)$ for FS decoding, and $(m_1=m_2=\cdots=m_{u'}=m; m_{u'+1}=m_{u'+2}=\cdots=m_u=0)$ for a RS scheme equipped with up to $u'$ preceding symbols. Also, in order to follow the track of past channel states (i.e., to preserve successive channel states information), $(m \geqq m_1 \geqq \cdots \geqq m_u \geqq 0)$. Accordingly, the number of states of the RS decoder, denoted $N'$ becomes

$$N'=N_e \cdot N'_{ch} \tag{6}$$

$$N'_{ch}=2^{\sum_{k=1}^{u} m_k} \tag{7}$$

where $N'_{ch}$ represents the number of channel reduced states. Evidently, $N'$ may vary from $N_e$ to $N$.[2),(3)] By the way, it can be observed that in the RS scheme of Fig. 2, $w=m-1$ (if $m_1=0$), or $w=m-m_1$ (if $m_1 \geqq 1$) bits will remain uncoded. In other words, the RS decoder trellis will have parallel transitions equal in number to $2^w$.

Besides, consider the alphabet $\mathcal{F}$ of the original mapper $F(\cdot)$ with cardinality $|\mathcal{F}|=2^{m+1}$. Then, the FS super-encoder mapper denoted $F_s(\cdot)$, with alphabet $\mathcal{F}_s$ of symbols corrupted by ISI will have a size given by $|\mathcal{F}_s|=|\mathcal{F}| \cdot |\mathcal{F}|^u=|\mathcal{F}| \cdot 2^{(m+1)u}=|\mathcal{F}| \cdot N_{ch} \cdot 2^u$ the same which, by reduction of the channel states $N_{ch}$, is as well diminished such that the cardinality of the RS super-encoder mapper, denoted $F'_s(\cdot)$, becomes $|\mathcal{F}'_s|=|\mathcal{F}| \cdot N'_{ch} \cdot 2^u$. Thus, by denoting with $p$ the number of non represented states per each state in the RS trellis, we get $p=N/N'=N_{ch}/N'_{ch}$, which in turn equals the number of non represented symbols, per each symbol in the RS trellis, since $|\mathcal{F}_s|/|\mathcal{F}'_s|=N_{ch}/N'_{ch}=p$. *These* $p$ symbols are to be estimated by the RS decoder as we will see next.

## 3. Transfer Function Bounds

### 3.1 Error Probability Analysis

Consider first the path metric recursively computed by the RS decoder

$$M_n(\alpha_n)=\min_{\{\alpha_{n-1}\} \to \alpha_n} \{M_{n-1}(\alpha_{n-1})+|\beta_n|^2\} \tag{8}$$

where the minimization is done according to the Viterbi algorithm over all the transitions defined between $\alpha_n$, a particular arriving state in the RS trellis, and its predecessors set $\{\alpha_{n-1}\}$. Also, $|\beta_n|^2$ is a squared distance branch metric, and the vector $\beta_n$ is expressed by

$$\beta_n=z_n-\sum_{k=0}^{u'} f_k s_{n-k}-\sum_{k=u'+1}^{u} f_k \hat{s}_{n-k}(\alpha_{n-1}) \tag{9}$$

wherein the last two terms arise from ISI. Since the decoder is assumed to have channel state knowledge for $u'$ preceding symbols, the last term corresponds to estimations, with estimated symbol at time $n-1$, $\hat{s}_{n-k}(\alpha_{n-1})$. For an $L$-length error event starting at time $n=0$ and ending at time $n=L$, and defined by the transmitted and decoded sequences $S_L$ and $S'_L$, respectively, the path leading to the starting state $\alpha_0$ will have symbol estimations, which may agree or not with the past transmitted symbols. Since the estimated symbols

are fed back for compensation of the unknown ones (operation called feedback equalization), the second possibility will affect following decisions producing what is meant by *error propagation effect* (when perfect agreement results, the error event would arise from the Gaussian ISI channel disturbances).

An error event will occur when the path metric of the correct path results larger than that of the incorrect path, which is expressed as

$$\Pr\left[M_L(\alpha_L) > M'_L(\alpha_L)\right] = \Pr\left[\sum_{n=1}^{L}(|\beta_n|^2 - |\beta'_n|^2) > 0\right] \tag{10}$$

We have just seen how successive branch metrics $|\beta_n|^2$ become dependent due to the feedback mechanism. This fact disables the attainment of transfer function bounds from the RS state transition diagram. In what follows, we overcome this difficulty and make the branch metrics independent by using the FS trellis diagram.

So far, we have seen that only some interfering symbols are included as labels of the RS trellis diagram, which is related to the fact that the RS decoder possess only partial information about the channel states. As well, it is known that in the FS trellis diagram, all the interfering symbols are included in the branch labels, which follows from the total channel state knowledge available to the FS decoder. Also, as we have seen in the previous section, there are $p$ symbols, per each symbol represented in the RS trellis, to be estimated by the RS decoder. Therefore, there are $p$ potential survivors that can influence the decision of the second and higher order error events.

Then, the fact that the number of possible survivors is the same than the unknown states, suggests that, in order to make them explicit, each one of the $N'$ reduced states can be combined with each of the $p$ unknown states. As a result, we obtain the $N$-state FS trellis diagram ($N'_p = N$), where each resultant transition contains in its symbol label one of the $p$ unknown past symbols, whereas each resultant state contains one of the $p$ unknown past states. The meaning difference between these labels and states, and those of the FS decoding case (in numbers they are identical), is that the formers represent feedback estimations, while the latters represent deterministic quantities. Like this, the utilization of the FS trellis (with yet some modifications), where branch metris are independent, will permit the derivation of transfer function bounds based on an $N$-state transition diagram. It also follows that the computational complexity will be the same for any $N'$-state RS scheme, since in any case we arrive to the $N$-state FS trellis.

We consider now the ocurrence of multiple error events as shown in Fig. 3, where the RS decoder cannot recognize the difference among the states $s_0, s_1, \cdots, s_{p-1}$, resultant from splitting of the RS states. Then, we express the error event probability as follows

$$P_E < \sum_{K=1}^{\infty}\sum_{L=1}^{\infty}\sum_{S_{K,L}}\sum_{S'_{K,L}} P_c[S_{K,L}]\sum_{i=0}^{p-1} P_K[s_i] \cdot \sum_{j=1}^{p-1} P[S_{K,L} \to S'_{K,L}/s_i \to s_j] \tag{11}$$

where the correct sequence is denoted by $S_{K,L}$ and its occurence probability by $P_c[S_{K,L}]$. The error events are classified by $K$, as first error event ($K=1$), second error event ($K=2$), and $M$-th error event ($K=M$). The length of each error event is represented by $L$. Also, $P_K[s_i]$ is the $K$-th error event starting state probability for $s_i$, and $P[S_{K,L} \to S'_{K,L}/s_i \to s_j]$ is the pairwise error probability for the incorrect path $S'_{K,L}$ starting from $s_i$ and ending at $s_j$ when such path exists, otherwise it is assumed to be zero. Then, if $s_0$ is assummed to be the transmitted state, the first error event will start from it at any time. Since at that moment there is no error event already in progress, $P_1[s_0]=1$ and $P_1[s_i]=0$ $(i=1, 2, \cdots, p-1)$. It follows then that the first error event term ($K=1$) in Eq. (11) will carry no error propagation effect, simply because the path leading to $s_0$ is the transmitted one. On the other hand, for $K \geqq 2$, the error events may start from any state $s_i$ but from $s_0$, since at that time at least one error event have already happened (i.e. $P_K[s_0]=0$ for $K \geqq 2$). It should be apparent that all the error event

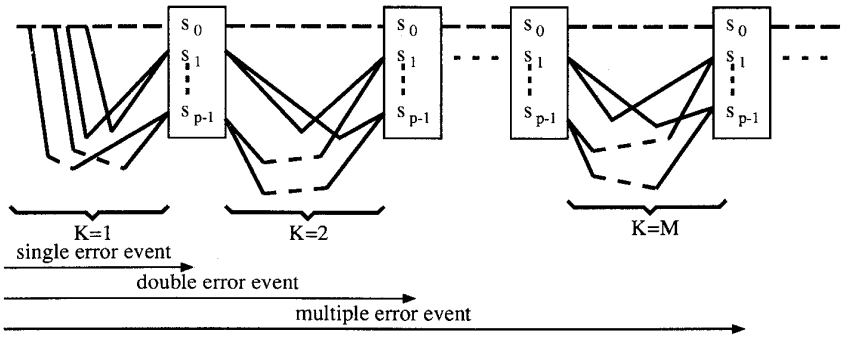


Fig. 3 Multiple error events.

terms from the second ($K \geqq 2$) in Eq. (11)) will contain the error propagation effect. Furthermore, all error events will end at any $s_i (i=1, 2, \cdots, p-1)$, where the exception made for $s_0$ is based on the general characteristic at the time of RS decision, where the transmitted state is not fully coincident with the decoded state (contrary to what happens in FS decoding). Then, we rewrite $P_E$ as

$$\begin{aligned} P_E < & \sum_{L=1}^{\infty} \sum_{S_{1,L}} \sum_{S'_{1,L}} P_c[S_{1,L}] \\ & \cdot \sum_{j=1}^{p-1} P[S_{1,L} \rightarrow S'_{1,L}/s_0 \rightarrow s_j] \Leftarrow (K=1) \\ & + \sum_{i=1}^{p-1} P_2[s_i] \sum_{L=1}^{\infty} \sum_{S_{2,L}} \sum_{S'_{2,L}} P_c[S_{2,L}] \\ & \cdot \sum_{j=1}^{p-1} P[S_{2,L} \rightarrow S'_{2,L}/s_i \rightarrow s_j] \Leftarrow (K=2) \\ & + \cdots \\ & + \sum_{i=1}^{p-1} P_M[s_i] \sum_{L=1}^{\infty} \sum_{S_{M,L}} \sum_{S'_{M,L}} P_c[S_{M,L}] \\ & \cdot \sum_{j=1}^{p-1} P[S_{M,L} \rightarrow S'_{M,L}/s_i \rightarrow s_j] \Leftarrow (K=M) \\ & + \cdots \end{aligned} \tag{12}$$

Before proceeding with the evaluation of Eq. (12), it is pertinent to note that induced by the ISI channel, the super-encoder of Fig. 2 has become non-uniform such that the all-zero transmitted sequence assumption[11] is no more valid. For this reason, we resort to the error weight matrix transfer function method,[12],[13] which is suitable for non-uniform schemes or sequence dependent error probability channels, and that deals with $N \times N$ matrix labels of the $N$-state transition diagram seen before. We prefer this method to the also general *pairwise-state* technique,[14] since the latter involves $N^2 \times N^2$ matrices.

Now, we define two transfer functions $\boldsymbol{T}_a(z)$ and $\boldsymbol{T}_b(z)$ in a matrix form, where $z$ is a parameter resulting from the Chernoff bound to be described in the next subsection. $\boldsymbol{T}_a(z)$ represents the transfer function of the first error event starting from $s_0$ and ending at $s_j$ $(j=1, 2, \cdots, p-1)$, while $\boldsymbol{T}_b(z)$ corresponds to the error events starting from $s_i$ and ending at $s_j (i, j=1, 2, \cdots, p-1)$. As shown in Ref. (13), each element $(i, j)$ of the transfer function matrix is an error event probability upper bound associated to the paths between $s_i$ and $s_j$, which in our case may be zero if $S'_{K,L}$ does not satisfy the condition $s_i \rightarrow s_j$. Both $\boldsymbol{T}_a(z)$ and $\boldsymbol{T}_b(z)$ are calculated by first obtaining the matrix labels $\boldsymbol{G}(e_n)$ of the $N$-state transition diagram correspondent to the $N$-state FS trellis, where $e_n$ denotes an error codeword of the super-encoder. An element of $\boldsymbol{G}(e_n)$ associated to a particular transition between states $p$ and $q$ is given by

$$[\boldsymbol{G}(e_n)]_{p,q} = \frac{1}{2^m} E[\exp \lambda \delta_n] \tag{13}$$

where $m$ is the number of input bits to the system, and $E[\cdot]$ denotes statistical expectation taken of the parameter $\lambda$ multiplied by $\delta_n$, which (we'll say for the moment) is related to the branch metrics. We observe that in Eq. (13), there's no summation taking account of parallel transitions, since in the FS trellis, upon the splitting of the RS trellis states, all transitions become singular. Also, we note that the following expression holds for the starting state probabilities

$$\begin{aligned} P_K[s_i] = & \sum_{k=1}^{p-1} P_{K-1}[s_k] \sum_{L=1}^{\infty} \sum_{S_{K-1,L}} \sum_{S'_{K-1,L}} \\ & \cdot P[S_{K-1,L} \rightarrow S'_{K-1,L}/s_k \rightarrow s_i] \\ & K \geqq 2 \end{aligned} \tag{14}$$

such that for the $K$-th error event, the starting probability for the state $s_i$ is given by adding the pairwise error probability of all the paths leading to it (for $K=1$ it was stated before that $P_1[s_0]=1$, and $P_1[s_i]=0$ for $i=1, 2, \cdots, p-1$). Then, we define new transfer function matrices $\boldsymbol{T}'_a(z)$ and $\boldsymbol{T}'_b(z)$ with elements $(i, j)$ containing the pairwise error (rather than the error event) probability upper bound for the paths starting at $s_i$ and ending at $s_j$. In this case, the elements of $\boldsymbol{G}(e_n)$ will be given by

$$[\boldsymbol{G}(e_n)]_{p,q} = E[\exp \lambda \delta_n] \tag{15}$$

where the factor $1/2^m$ is dropped since in Eq. (14) the probability of the correct sequence given by $P_c[S_{K,L}] = (1/2^m)^L$ needs not to be included. Using these defined transfer function matrices, we rewrite the error event probability as

$$P_E < \frac{1}{N} \mathbf{1} \cdot \boldsymbol{T}(z) \cdot \mathbf{1}^T \tag{16}$$

where $\boldsymbol{T}(z)$ denotes the total transfer function matrix, $\mathbf{1}$ is a $N$-dimensional row vector all of whose elements are 1, and $\mathbf{1}^T$ denotes its transpose. It follows that $\boldsymbol{T}(z)$ is given as

$$\begin{aligned} \boldsymbol{T}(z) = & \boldsymbol{T}_a(z) \Leftarrow (K=1) \\ & + \boldsymbol{T}'_a(z)\, \boldsymbol{T}_b(z) \Leftarrow (K=2) \\ & + \cdots \\ & + \boldsymbol{T}'_a(z)\, \boldsymbol{T}'^{M-2}_b(z)\, \boldsymbol{T}_b(z) \Leftarrow (K=M) \\ & + \cdots \end{aligned} \tag{17}$$

$$\boldsymbol{T}(z) = \boldsymbol{T}_a(z) + \boldsymbol{T}'_a(z)[\boldsymbol{I} - \boldsymbol{T}'_b(z)]^{-1} \boldsymbol{T}_b(z) \tag{18}$$

where $\boldsymbol{I}$ denotes the $N \times N$ identity matrix. An illustrative example of the defined transfer function matrices will be given in Sect. 3.3.

Now, in order to obtain the bit error probability upper bound, we extend $\boldsymbol{T}_a(z)$ and $\boldsymbol{T}_b(z)$ to include the number $\varepsilon$ of incorrect input bits. The extended

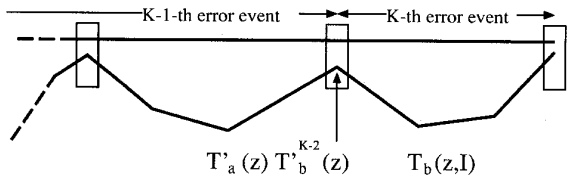


Fig. 4 Starting state probability.

transfer functions are denoted $\boldsymbol{T}_a(z, I)$ and $\boldsymbol{T}_b(z, I)$, where $I$ is an indeterminate whose exponent is $\varepsilon$. Then, the total transfer function is extended to $\boldsymbol{T}(z, I)$. Using the fact that the pairwise error probability is multiplied by the number of incorrect input bits in $\partial \mathbf{1} \cdot \boldsymbol{T}(z, I) \cdot \mathbf{1}^T / \partial I|_{I=1}$, and from Eqs. (16) and (18), we get

$$P_b < \frac{1}{mN} \left. \frac{\partial \mathbf{1} \cdot \boldsymbol{T}(z, I) \cdot \mathbf{1}^T}{\partial I} \right|_{I=1} \tag{19}$$

where

$$\boldsymbol{T}(z, I) = \boldsymbol{T}_a(z, I) + \boldsymbol{T}'_a(z)[\boldsymbol{I} - \boldsymbol{T}'_b(z)]^{-1} \boldsymbol{T}_b(z, I) \tag{20}$$

Figure 4 shows the $K$-th error event ($K \geqq 2$), whose starting state probability is given by $\boldsymbol{T}'_a(z)\, \boldsymbol{T}'^{K-2}_b(z)$. For convenience, the bound of Eq. (19) will be called the Union Bound (UB).

### 3. 2 Chernoff Bound

We will see now how the elements $[\boldsymbol{G}(e_n)]_{p,q}$ of the matrix labels needed for the computation of the transfer function matrices $\boldsymbol{T}_a(z)$, $\boldsymbol{T}_b(z)$, $\boldsymbol{T}'_a(z)$ and $\boldsymbol{T}'_b(z)$ given by Eqs. (13) and (15) respectively, are derived. We make

$$P[S_{K,L} \rightarrow S'_{K,L} / s_i \rightarrow s_j] = \Pr\left[\sum_{n=1}^{L} \delta_n > 0\right] \tag{21}$$

$$\delta_n = |\beta_n|^2 - |\beta'_n|^2 \tag{22}$$

where $|\beta_n|^2$ and $|\beta'_n|^2$ are the squared distance branch metrics of $S_{K,L}$ and $S'_{K,L}$ respectively, as shown in Eq. (10). Then, with $\gamma_n$ and $\gamma'_n$ representing the correct and incorrect signal vectors (associated to the FS trellis transition labels) respectively, and with $\eta_n$ as the noise vector, we rewrite $\delta_n$ as

$$\delta_n = |\eta_n|^2 - |\gamma_n + \eta_n - \gamma'_n|^2 \tag{23}$$

$$= -2(\gamma_n - \gamma'_n) \cdot \eta_n - |\gamma_n - \gamma'_n|^2 \tag{24}$$

$$= a_n x_n + b_n y_n + c_n \tag{25}$$

where

$$a_n = -2(r_{xn} - r'_{xn}) \tag{26}$$

$$b_n = -2(r_{yn} - r'_{yn}) \tag{27}$$

$$c_n = -|\gamma_n - \gamma'_n|^2 \tag{28}$$

In turn $(x_n, y_n)$, $(r_{xn}, r_{yn})$ and $(r'_{xn}, r'_{yn})$ are the coordinates of the vectors $z_n$, $\gamma_n$ and $\gamma'_n$, respectively. Then, by applying the Chernoff bound to Eq. (21), we get

$$P[S_{K,L} \rightarrow S'_{K,L} / s_i \rightarrow s_j]$$

$$= P\left[\sum_{n=1}^{L} \delta_n > 0\right] \tag{29}$$

$$\leqq E[\exp \lambda \sum_{n=1}^{L} \delta_n] = \prod_{n=1}^{L} E[\exp \lambda \delta_n] \tag{30}$$

and

$$E[\exp \lambda \delta_n] = \int_{-\infty}^{\infty} \int_{-\infty}^{\infty} e^{\lambda(ax+by+c)} p_G(x, y)\, dxdy \tag{31}$$

where $\lambda$ is the Chernoff parameter to be optimized, and $p_G(x, y)$ represents the Gaussian noise probability density function (pdf). Equation (30) holds for memoryless channels in general, while Eq. (31) considers the particular case of Gaussian memoryless channel or Gaussian ISI channel rendered as ISI-free owing to the super-encoder configuration. After simplification (dropping the time subindex $n$)

$$E[\exp \lambda \delta_n] = e^{\lambda(ar_x + br_y + c)} e^{\frac{\lambda^2}{2}(a^2+b^2)\sigma^2} \tag{32}$$

where $\sigma^2$ denotes the noise power. Optimization of Eq. (32) over $\lambda$ gives

$$\frac{dE[\exp \lambda \delta_n]}{d\lambda} = 0 \tag{33}$$

$$\lambda = \frac{1}{4\sigma^2} \tag{34}$$

Then, by replacing the optimum value of $\lambda$ in Eq. (32) we obtain

$$E[\exp \lambda \delta_n] = e^{-\frac{1}{8\sigma^2}|\gamma_n - \gamma'_n|^2} = z^{|d_n|^2} \tag{35}$$

where $d_n$ is the branch distance vector between $\gamma_n$ and $\gamma'_n$ (shown later in Fig. 7) and $z = e^{-1/8\sigma^2}$. Finally, upon the obtention of all the matrix labels $\boldsymbol{G}(e_n)$, the transfer function can be computed. In this paper, we have calculated $\boldsymbol{T}(z, I)$ following Ref. (15), by a series expansion approach.

### 3. 3 Example

We wish now to illustrate the transfer function bounds by a simple example. We consider the case where $m=1$, $\nu=2$ and $u=1$ in Fig. 2, for an RS scheme with $m_1=0$, $u'=0$. The resultant $N=4$-state super-encoder, $N'=2$-state RS and $N=4$-state FS trellises are shown in Figs. 5(a), (b) and (c) respectively, and the FS state diagram in Fig. 5(d). The RS Viterbi decoder will estimate then, $p=4/2=2$ symbols (or states) per each symbol (or state) represented in the RS trellis. The parameters denoted $\tau_n$ and $\pi_n$ reveal one of two states of a binary encoder and of an ISI

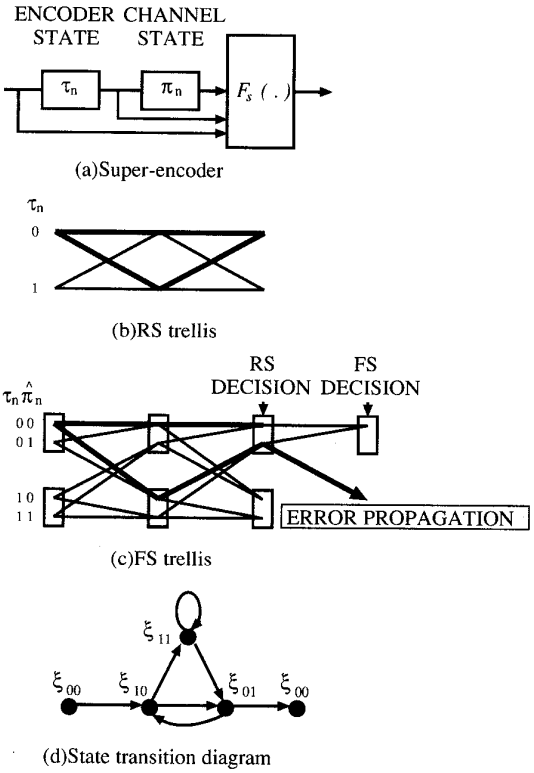


Fig. 5 RS decoding error event (example).

channel, respectively. While in the trellis for FS decoding the combination of encoder and channel states produce the set denoted $\{\tau_n\pi_n$:$00(\xi_{00})$, $01(\xi_{01})$, $10(\xi_{10})$, $11(\xi_{11})\}$, in the FS trellis intended for RS transfer function bounds calculation, the same set is obtained but from the combination of $\tau_n$ and the estimated channel states denoted $\hat{\pi}_n$. In Figs. 5(b) and (c), an example of an RS first error event is highlighted by thick lines. Then

- Since the RS Viterbi decoder possess no information about the ISI states (Fig. 5(b)), it can be said that at the time of RS decision (Fig. 5(c)), the states 00 and 01, on one side, and, the states 10 and 11 on the other, will be seen the same from the RS decoder point of view. With the aim of error event probability analysis and computation, we consider all the combinations arising from the known states and channel state estimations, thus becoming necessary a 4-state transition diagram.
- In Fig. 5(c), with the assumption that the upper sequence following the 00 states route is the correct, once the incorrect sequence reaches 01, for the RS decoder the error event is considered to be ended. In such case, the ISI state may become correct with the transition leading to 00 (meaning that no error event happens next), otherwise error propagation will repeatedly occur by the transition leading to 10.

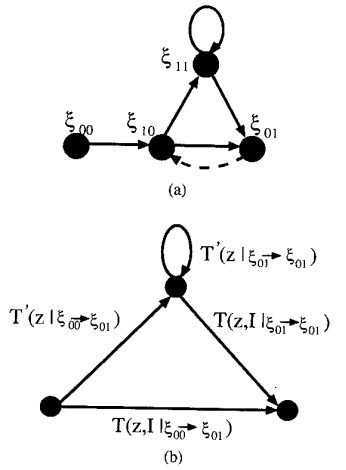


Fig. 6 RS transfer function (example).

- At the time of RS decision, the transmitted state 00 is not fully coincident with the decoded state 01 which is in contrast with the total coincidence at the time of FS decision. Here, the RS decisions are taken prematurely if compared with FS decoding. In general however, an error event length in the RS trellis may be shorter or equal to that of the FS trellis, depending on the particular RS scheme's complexity.

With the above characterization, the RS Viterbi decoding transfer function can be obtained as follows. First, by considering $\xi_{01}$ in Fig. 5(d) a terminating state, we have a state transition diagram as shown in Fig. 6(a). Then, since the RS decoder ignores the channel states, for an error event diverging at $\xi_{00}$, a decision will be made when it passes for the first time by $\xi_{01}$. Now, this error event probability multiplied by the number of input error bits along the associated path, gives the bit error probability. However, the dotted line transition going from $\xi_{01}$ to $\xi_{10}$ can be thought as a new error event starting from the just ended one. This new error event will proceed with pairwise error probability already attained up to $\xi_{01}$, while a new count of input error bits is started, thus passing once more by $\xi_{01}$. Like this, new error events end and start again indefinitely.

Now, let $\boldsymbol{T}(z, I/\xi_{00}\to\xi_{01})$ and $\boldsymbol{T}'(z/\xi_{00}\to\xi_{01})$ denote the first error event transfer function matrices correspondent to $\boldsymbol{T}_a(z, I)$ and $\boldsymbol{T}_a'(z)$ in Eq. (11) respectively. Let also $\boldsymbol{T}(z, I/\xi_{01}\to\xi_{01})$ and $\boldsymbol{T}'(z/\xi_{01}\to\xi_{01})$ represent the transfer function matrices correspondent to $\boldsymbol{T}_b(z, I)$ and $\boldsymbol{T}_b'(z)$ in Eq. (11) respectively. Thus, the total transfer function matrix can be written as follows

$$\boldsymbol{T}(z, I)=\boldsymbol{T}(z, I/\xi_{00}\to\xi_{01})+\boldsymbol{T}'(z/\xi_{00}\to\xi_{01})\cdot[\boldsymbol{I}-\boldsymbol{T}'(z/\xi_{01}\to\xi_{01})]^{-1}$$

$$\cdot T(z, I/\xi_{01} \rightarrow \xi_{01}) \qquad (36)$$

which is shown in an equivalent state transition diagram in Fig. 6(b).

## 4. Tighter Bounds

When Viterbi decoding takes place in a trellis with parallel transitions, a decoded branch symbol is, among the members of the parallel transition, the nearest in Euclidean distance to the received signal $z_n$. This feature is not exclusive of TCM systems, since also uncoded schemes with RS decoding based on set partitioning principles may have parallel transition trellises.[1] Conventional coded schemes (for instance, convolutionally encoded Binary PSK), can be decoded also in a similar fashion. Then, even though the usual pairwise error probability of Eq. (10), based on the path metric condition,

$$P[S_{K,L} \rightarrow S'_{K,L}/s_i \rightarrow s_j] = \Pr[M_L(\alpha_L) > M'_L(\alpha_L)] \qquad (37)$$

holds equally for decoding on trellises with or without parallel transitions, in the former case and from the above argument we can write

$$P[S_{K,L} \rightarrow S'_{K,L}/s_i \rightarrow s_j] = \Pr[M_L(\alpha_L) > M'_L(\alpha_L) \text{ and } M'_n(\alpha_n) < M''_n(\alpha_n),\ n=1, 2, \cdots, L] \qquad (38)$$

where the condition $M'_n(\alpha_n) < M''_n(\alpha_n)$ expresses the fact that a branch which forms part of the decoded sequence $S'_{K,L}$ possess the smallest metric $M'_n(\alpha_n)$ among the members of the parallel transition. Like this, we make explicit the two conditions satisfied by a sequence decoded in such a trellis. In turn, $M''_n(\alpha_n)$ denotes the branch metric associated to any other sequence diverging from the decoded $S'_{K,L}$, called $S''_{K,L}$ hereafter, resultant from parallel transitions concatenation. Define now the set $E'_L$ of $k_L$ error patterns defining all the sequences $S''_{K,L}$, given by $E'_L = \{E_L(1), E_L(2), \cdots, E_L(k_L)\}$. Thus, we obtain, by union of the above patterns, the following upper bound

$$P[S_{K,L} \rightarrow S'_{K,L}/s_i \rightarrow s_j] < \sum_{i=1}^{k_L} P[S_{K,L} \rightarrow S'_{K,L}/s_i \rightarrow s_j | E_L(l)] \qquad (39)$$

with

$$P[S_{K,L} \rightarrow S'_{K,L}/s_i \rightarrow s_j | E_L(l)] = \Pr[M_L(\alpha_L|E_L(l)) > M'_L(\alpha_L|E_L(l)) \text{ and } M'_n(\alpha_n|E_L(l)) < M''_n(\alpha_n|E_L(l)),\ n=1, 2, \cdots, L] \qquad (40)$$

In distance metric terms,

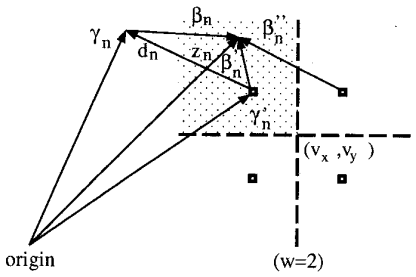


$2^w = 4$ decision regions

▫ : symbol assigned to a parallel transition

Fig. 7 Parallel transitions decision space.

$$P[S_{K,L} \rightarrow S'_{K,L}/s_i \rightarrow s_j | E_L(l)] = \Pr\left[\sum_{n=1}^{L}(|\beta_n|^2 - |\beta'_n|^2) > 0 \text{ and } \sum_{n=1}^{J}(|\beta'_n|^2 - |\beta''_n|^2) < 0,\ J=1, 2, \cdots, L\right] \qquad (41)$$

wherein $|\beta''_n|^2$ is the branch metric for the $S''_{K,L}$ sequences. The received signal vector $z_n$ will lie then, in one of the decision regions defined by the $2^w$ parallel transitions, depending on the noise vector $\eta_n$. Figure 7 illustrates such a situation when the uncoded number of bits in the RS scheme is $w=2$. As shown, the received signal $z_n$ lies nearest to one of the four symbols assigned to the parallel transitions. Therefore, the branch metric of Eq. (41) can be obtained only from the involved decision region, or by considering a *truncated* instead of complete Gaussian noise pdf. We apply the Chernoff bound for the particular case of Fig. 7, since in general the expectation integral limits will depend on how the decision space is divided, according to the number of parallel transitions of the particular RS decoding trellis. Then

$$E[\exp \lambda\delta_n] = \int_{-\infty}^{\infty}\int_{-\infty}^{\infty} e^{\lambda(ax+by+c)} p_T(x, y)\, dxdy = \int_{y_1}^{y_2}\int_{x_1}^{x_2} e^{\lambda(ax+by+c)} p_G(x, y)\, dxdy \qquad (42)$$

where $p_T(x, y)$ represents the truncated Gaussian noise pdf. After simplification, we obtain

$$E[\exp \lambda\delta_n] = e^{\lambda(ar_x+br_y+c)} e^{\frac{\lambda^2}{2}(a^2+b^2)\sigma^2} \cdot \begin{cases} Q[h_x(\lambda)] \cdot Q[h_y(\lambda)] & \text{if } r'_x > v_x,\ r'_y > v_y \\ Q[h_x(\lambda)] \cdot (1 - Q[h_y(\lambda)]) & \text{if } r'_x > v_x,\ r'_y < v_y \\ (1 - Q[h_x(\lambda)]) \cdot (1 - Q[h_y(\lambda)]) & \text{if } r'_x < v_x,\ r'_y < v_y \\ (1 - Q[h_x(\lambda)]) \cdot Q[h_y(\lambda)] & \text{if } r'_x < v_x,\ r'_y > v_y \end{cases} \qquad (43)$$

where $h_x(\lambda)=(v_x-r_x/\sigma)-\lambda a\sigma$, $h_y(\lambda)=(v_y-r_y/\sigma)-\lambda b\sigma$, and $(v_x, v_y)$ denotes the truncation point (see Fig. 7) (each case corresponds to a decision region). $Q[\cdot]$ stands for the $Q$ function given by $Q(x)=(1/\sqrt{2\pi})\int_x^\infty e^{-t^2/2}dt$. Concerning the Chernoff parameter $\lambda$, in this case it cannot be obtained an optimum value independent of time, as that for the complete pdf case given by Eq. (34). Therefore, upon the calculation of the bit error probability upper bound as a function of $\lambda$, numerical optimization of the same will be necessary. The tighter bound that arises from an element taken from the union bound at the RHS in Eq. (39), will be called the Elementary Bound (EB), to distinguish it from the UB given by Eq. (19). Then, the EB becomes

$$P_b<\min_{\lambda\geq 0}\frac{1}{mN}\left.\frac{\partial \mathbf{1}\cdot \boldsymbol{T}(z', I)\cdot \mathbf{1}^T}{\partial I}\right|_{I=1} \tag{44}$$

In this case, due to the pdf truncation $z'=e^{-(\lambda-2\lambda^2\sigma^2)}(z'$ reduces to $z$ of Eq. (35) when $\lambda=1/4\sigma^2$).

For the cases where the Chernoff bound is not satisfactory enough, yet another approach, by moments, could prove useful. A moment bound is optimum in the sense that from the moment information of the r.v. ($\delta$ in this case), it cannot be further tightened.[16] In Ref. (17) we derive such moment bound and discuss an algorithmic approach for computing the bit error probability $P_b$.

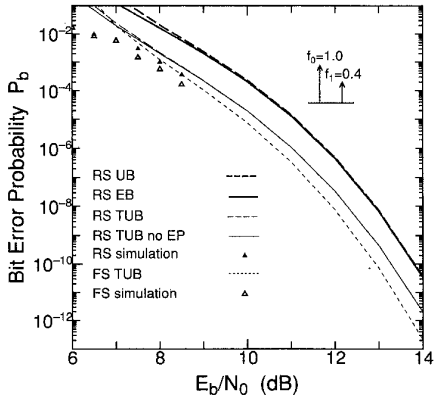


Fig. 8 16-QAM TCM system RS performance.

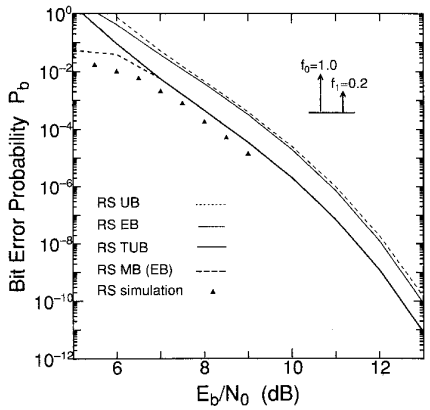


Fig. 9 16-QAM TCM system RS performance.

## 5. Results

The simulation and theoretical performance in terms of bit error probability $P_b$ vs. bit energy to noise ratio $E_b/N_0$ ($N_0=2\sigma^2$ denotes one sided noise power spectral density) of the $N_e=4$-state 16-QAM TCM scheme in a $u=1$-symbol ISI channel are shown below. With $m=3$ and $m_1=0$, the RS decoder trellis has $N'=N_e=4$ states with $2^{3-1}=4$ parallel transitions. The associated FS trellis has $N=4\cdot 8=32$ states. In Fig. 8 we show the different bounds obtained by Chernoff. The elementary bound (EB) coming from the truncated pdf, is shown tighter than the union bound (UB) which is derived from the complete pdf. Its tightness however, will depend in general on the number of elements which conform the union bound. On the other hand, the tight upper bound (TUB)[18] shows even tighter, but it is attainable only for the complete pdf Gaussian noise model or UB. All the bounds include the effect of error propagation (EP) unless otherwise indicated. It is noted that whereas the EP effect is noticeable in the low $E_b/N_0$ region, since error events occur more frequently for higher noise levels, in the case of moderate and high $E_b/N_0$ ratios, the bound is dominated by the Gaussian ISI channel impairments.

In Fig. 9 the moments bound (MB) correspondent to the (EB) is given up to 7 dB, since roundoff errors prevent the computation for higher $E_b/N_0$ ratios. The trellis (based on pair states) employed in the algorithmic calculation has $N^2=1024$ states.[17] In all the cases, 12 moments were considered and moments convolution was performed 7 times. It is hopeful that by increasing the number of moments, a tighter bound might be obtained, but for the present scheme, we haven't go further due to excessive computing time.

## 6. Conclusions

We have presented a novel theoretical analysis for RS schemes employing Viterbi decoding. New error probability transfer function bounds have been derived for RS schemes by employing the FS trellis diagram, while this has served as a way to include the error propagation effect. Also, a tighter bound has been obtained for RS decoding schemes having parallel transitions. Such bound is not only applicable to TCM, but in general to any RS scheme based on set partitioning principles. Computationally, the Chernoff bound and the so called tight upper bound (TUB) have been applied with the transfer function, to

obtain the ultimate bound of interest, the bit error probability upper bound.

## Acknowledgment

This work was partially supported by a grant in aid of Fujitsu Laboratories Ltd. The authors wish to thank H. Nakamura, General Deputy Manager, T. Takano, Deputy Manager, and E. Fukuda, Section Manager of the Communication and Space Div., Fujitsu Laboratories Ltd., for the support.

### References

(1) Eyuboglu, M. V. and Qureshi, S. U., "Reduced-State Sequence Estimation with Set Partitioning and Decision Feedback," *IEEE Trans. Commun.*, vol. COM-36, no. 1, pp. 13-20, Jan. 1988.

(2) Chevillat, P. R. and Eleftheriou, E., "Decoding of Trellis-Encoded Signals in the Presence of Intersymbol Interference," *IEEE Trans. Commun.*, vol. COM-37, no. 7, pp. 669-676, Jul. 1989.

(3) Eyuboglu, M. V. and Qureshi, S. U., "Reduced-State Sequence Estimation for Coded Modulation on Intersymbol Interference Channels, *IEEE J. Sel. Areas Commun.*, vol. SAC-7, no. 6, pp. 989-995, Aug. 1989.

(4) Duel-Hallen, A. and Heegard, C., "Delayed Decision Feedback Sequence Estimation," *IEEE Trans. Commun.*, vol. COM-37, no. 5, pp. 428-436, May 1989.

(5) Forney, Jr., G. D., "Maximum Likelihood Sequence Estimation of Digital Sequences in the Presence of Intersymbol Interference," *IEEE Trans. Inf. Theory.*, vol. IT-18, no. 3, pp. 368-378, May 1972.

(6) Foschini, G. J., "Performance Bound for Maximum Likelihood Reception of Digital Data," *IEEE Trans. Inf. Theory*, vol. IT-21, no. 1, pp. 47-50, Jan. 1975.

(7) Ungerboeck, G., "Adaptive Maximum Likelihood Receiver for Carrier Modulated Data Transmission Systems," *IEEE Trans. Commun.*, vol. COM-22, no. 5, pp. 624-636, May 1974.

(8) Qureshi, S. U., "Adaptive Equalization," *Proceedings of the IEEE*, vol. 73, no. 9, pp. 1349-1387, Sep. 1985.

(9) Sheen, W. H. and Stuber, G. L., "Error Probability of Reduced State Sequence Estimation," *IEEE J. Sel. Areas Commun.*, vol. SAC-10, no. 3, pp. 571-578, Apr. 1992.

(10) Ungerboeck, G., "Channel Coding with Multilevel/Phase Signals," *IEEE Trans. Inf. Theory*, vol. IT-28, no. 1, pp. 55-67, Jan. 1982.

(11) Viterbi, A. J., "Convolutional Codes and Their Performance in Communication Systems," *IEEE Trans. Commun.*, vol. COM-19, no. 5, pp. 751-772, Oct. 1971.

(12) Oka, I. and Biglieri, E., "Error Probability Bounds for Trellis Coded Modulation over Sequence Dependent Channels," *Trans. IEICE*, vol. E72, no. 4, pp. 375-383, Apr. 1989.

(13) Liu, Y. J., Oka, I. and Biglieri, E., "Error Probability for Digital Transmission Over Nonlinear Channels with Application to TCM," *IEEE Trans. Inf. Theory*, vol. IT-36, no. 5, pp. 1101-1110, Sep. 1990.

(14) Omura, J. K. and Simon, M. K., *Modulation/Demodulation Techniques for Satellite Communications, Part IV: Appendices*, JPL Publication 81-73, Nov. 1981.

(15) Oka, I., Liu, Y. J. and Biglieri, E., "Error Matrix and Pairwise-State Methods in the Error Probability Analysis of Trellis Coded Modulation," *Trans. IEICE*, vol. J73-B-I, no. 12, pp. 939-947, Dec. 1990.

(16) Benedetto, S., Biglieri, E., Luvison, A. and Zingarelli, V., "Moment Based Performance Evaluation of Digital Transmission Systems," *IEE Proceedings-I*, vol. 139, no. 3, pp. 258-266, Jun. 1992.

(17) Valdez, C., Fujiwara, H., Oka, I. and Yamamoto, H., "Error Probability Analysis in Reduced State Viterbi Decoding," *IEICE Technical Report*, IT92-69, Aug. 1992.

(18) Benedetto, S., Marsan, M. A., Albertengo, G. and Giachin, E., "Combined Coding and Modulation: Theory and Applications," *IEEE Trans. Inf. Theory*, vol. IT-34, no. 2, pp. 223-236, Mar. 1988.

**Carlos Valdez** was born in Lima, Peru, on September 15, 1956. He received his B. Sc. degree in Electrical Eng. from the Universidad Nacional de Ingeniería in Lima, Peru, in 1981, after which he joined the Instituto Nacional de Investigación y Capacitación de Telecomunicaciones (INICTEL). From 1985 to 1988 he was a lecturer at the Universidad Nacional Mayor de San Marcos. As a recipient of a scholarship from the Ministry of Education and Culture of Japan, he joined the University of Electro-Communications in Tokyo, and received the M. Eng. degree in Electrical Eng. in 1991. Currently, he is working towards the D.Eng. degree with research interests involving coding and modulation systems performance analysis.

**Hiroyuki Fujiwara** was born in Kanagawa, Japan, on February 5, 1967. He received the B. E. and M. E. degrees in electrical engineering from University of Electro-Communications, Tokyo, in 1990 and 1992 respectively. Since 1992, he has been studying for the Ph. D. at the Communications and Systems Department, University of Electro-Communications. He is engaged in research on communication theory. He is a student member of the Institute of Electrical and Electronics Engineers (IEEE).

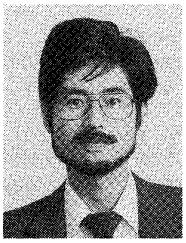

**Ikuo Oka** was born in Hyogo, Japan, on August 11, 1955. He received the B. S., M. Eng., and D. Eng. degrees in communication engineering from Osaka university, Osaka Japan, in 1978, 1980 and 1983, respectively. In 1983 he joined the Faculty of the University of Electro-Communications, Tokyo, first as an Assistant Professor, then as an Associate Professor. Since April 1991 he has been an Associate Professor at the Department of Information and Computer Science, Faculty of Engineering, Osaka City University, Osaka. In 1988-1989 he was a Visiting Scholar at the Electrical Engineering Department, UCLA, Los Angeles. His current interests include coding and modulation in satellite and optical communications. Dr. Oka is a member of IEEE and SITA.

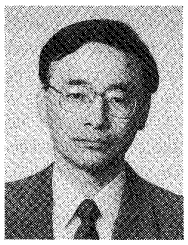

**Hirosuke Yamamoto** was born in Wakayama, Japan, on November 15, 1952. He received the B. E. degree from Shizuoka University, Shizuoka, Japan, in 1975 and the M. E. and Dr. E. degrees from the University of Tokyo, Tokyo, Japan, in 1977 and 1980, respectively, all in electrical engineering. In 1980 he joined Tokushima University, Tokushima, Japan. He was an Associate Professor at Tokushima University from 1983 to 1987 and at the University of Electro-Communications, Tokyo, Japan, from 1987 to 1993. Since 1993 he has been an Associate Professor in the Department of Mathematical Engineering and Information Physics, Faculty of Engineering, the University of Tokyo, Tokyo, Japan. In 1989-90, he was a Visiting Scholar at the Information Systems Laboratory, Stanford University. His research interests are in Shannon theory, coding theory, and cryptography. Dr. Yamamoto is a member of the IEEE.